DYNAMIC SIMULATIONS OF SUPERCONDUCTING QUANTUM INTERFERENCE DEVICE (SQUID) MEMORY CELL

ABSTRACT

A thorough investigation has been made to obtain SQUID device parameters and properties, and the optimization of the latter for the application of memory cells. The SQUID memory cells have been designed theoretically using the optimized techniques. Our concept of turn-on delay has been applied for critically ascertaining the switching speed of the logic gates and memory cells. The dynamic response of the memory cells have been obtained by computer-simulation. This paper helps scientists and researchers in giving complete understanding of SQUID memory cells before they are fabricated experimentally.

***Keywords*—Superconducting electronics, SQUIDMemory Cell, Dynamic Simulations**

1. INTRODUCTION

Josephson junction alone cannot be used as a logic gate since it lacks isolation, i.e., the output signal can propagate in the input as well as in the output branches, whereas for logic operation the signal must propagate only in the output branches. The other problem with this circuit is that the output current is not sufficient to switch more than one load. High-gain Josephson logic devices are desired for many reasons: first, they provide higher fan-out capability (fan-out means the number of loads). Second, high-gain to some extent can be traded off to improve the circuit tolerances variations in processing parameters such as critical currents. Finally, high-gain would result in shorter gate delays because of the shorter turn-on delays [1] and the shorter time required for signal currents to reach the device threshold. In practice, a gain of 3 is found to be optimum for Josephson logic circuits. At gains much larger than 3, there is no significant improvements in the gate delay but, on the other hand, the noise margins for the "0" state degrades considerably

1. Dr. K.SRINIVAS DEPARTMWENT OF PHYSICS, GMR INSTITUTE OF TECHNOLOGY, RAJAM-532127,A.P., INDIA
Email : srinkura@gmail.com srinivas.k@gmrit.org

.

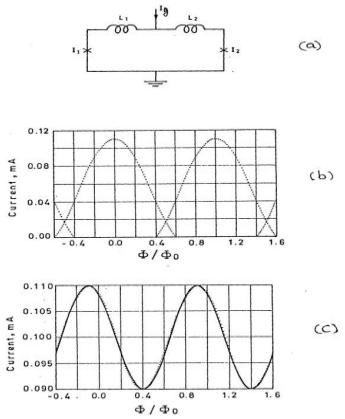

Fig. 1 (a) Diagram of a dc SQUID with bias current. The inductances and junctions on the two sides may be different. The crosses represent the junctions, including resistances and capacitances.

(b) The positive half of the threshold characteristic of a symmetric dc SQUID having L1 = L2 = 2.0 pH and I1 = I2 = 55 μA.(c)The positive portion of the threshold characteristic of an asymmetric dc SQUID with L1 = L2 = 2.0 pH and I1 = 100μA ; I2= 10μA.

Further, the quantum-mechanical nature of superconductivity provides a natural mechanism for the storage of digital information. If a current is established in a loop of superconductor, it generates a magnetic field that passes through the center of the loop. The direction of the field is determined by the direction of the current. The magnitude of the magnetic field (due to the current) is quantized, that is, it can assume only certain discrete values, and if it changes, it does so only by jumping from one allowed value to another. What is more, both the current and magnetic field are persistent, and they remain unchanged even after the driving current is removed. Information can be stored in such loops by letting one quantized state to a binary "1" and the other to a binary "0".
The Superconducting Quantum Interference Device

(SQUID) is a device which can be used for both logic and memory applications. It consists of two Josephson junctions coupled by two inductors as shown in Fig.1a The two most attractive features of SQUID devices for logic applications are isolation and serially connected fan-out. The isolation is provided by the transformer coupling between the SQUID and the input. The other advantage of SQUID is the serial fan-out capability whereby the control lines of many load devices can be connected in series with a single output line.

Since the SQUID is in the form of a loop, it can be utilized for memory purpose. Information can be stored in the form of single-flux quantum [2] [3] [4].

Since the present thesis deals with the design of logic gates and memories using the SQUID, it is necessary to have a detailed information regarding the parameters, properties and their optimization for the application of logic and memory cell. In fact, in the present chapter we have made an attempt on this line.

2. BRIEF THEORY OF DC SQUID

The Superconducting Quantum Interference Device (SQUID) consists of two Josephson junctions coupled by inductors as shown in Fig.1a. The supercurrent Ig passing through a single junction from a superconductor to the other can be expressed as a function of θ the gauge-invariant phase difference between the order parameters of the bulk superconductors on either side of the barrier. The net transport supercurrent Ig carried by the junction is [5],

$Ig = Io1 \sin\theta1 + Io2 \sin\theta2$ -----(1)

Further, there is the usual constraint on the difference between $\theta1$ and $\theta2$, namely,

$\theta2 - \theta1 = 2\pi \phi / \phi o$ ----------(2)

where ϕ is the total magnetic flux, which is the sum of two parts, the first denoted by Ix, comes from the applied magnetic field or current, and the second Is is the magnetic flux set by the flow of current I1 and 12 which can be written as,

$\phi s = L1 I1 – L2 I2$ ---------- (3)

where L1 and L2 are the self-inductances of the line. The sum of L1 and L2 is equal to L, the total inductance of the loop.

From (2) and (3),

$\theta2 - \theta1 = 2\pi Ix / Io + 2\pi L1 I1 / Io - 2\pi L2. I2 / \phi o$ ----------(4)

Egn.(4) can be rewritten as,

$\phi x / \phi o = \theta2 - \theta1 + \beta2. \sin\theta2 - \beta1 . \sin\theta1 + 2\pi N$ ---------- (5)

where $\beta i = Li . Ioi / \phi o$; $\beta = .\beta2 + \beta1 . Io2 / Io1$ --- (6)

The phase angles $\theta1$ and $\theta2$ at the vortex boundaries are obtained from stability consideration and represented by a simple expression,

$$\cos\theta_2 = \frac{-\cos\theta_1}{(I_{o2}/I_{o1} + \beta\cos\theta_1)} \quad \text{-----(7)}$$

where Io1 and Io2 are the critical currents of the Josephson junctions J1 and J2 respectively.

To construct the mode boundaries [4] [6-8], one phase angle is used as an independent parameter. The stability equation is then solved for the other phase and both are inserted into the equation for Ig and ϕ. To obtain a full mode boundary, a convenient choice for the phase angle $\theta1$ and $\theta2$ as follows:

(a) $\theta1$ is independent and varies between -90 and +90. The stability equation is solved for two solutions of $\theta2$ with values restricted to the range -180 and +180. This yields one half of the vortex boundary.

(b) The second half is obtained as before but $\theta1$ is replaced by $\theta2$ as an independent variable.

We now make a few observations about the double-junction interferometers which usually relates to measurable features, and from which the junction parameters may be deduced.

(1) $\theta1 = \theta2 = + 1/2\ \pi$ are always solutions, even for asymmetric feeds or critical currents, as Eqn (7) shows. For these phase, Ig = + (Io1 + Io2). Thus the maximum current is always the sum of the junction critical currents, which is not the case with a three-junction interferometer.

Also, $\phi x = + (L2\ Io2 - L1\ Io1) + N\ \phi o$, at this extream. Measurement of relative displacement of the minimum and maximum of Ig thus provides one measure of the asymmetry.

(2) The double-junction interferometers can exhibit nearly sinusoidal Ig (ϕ) behaviour (as shown in Fig.2) when [8],

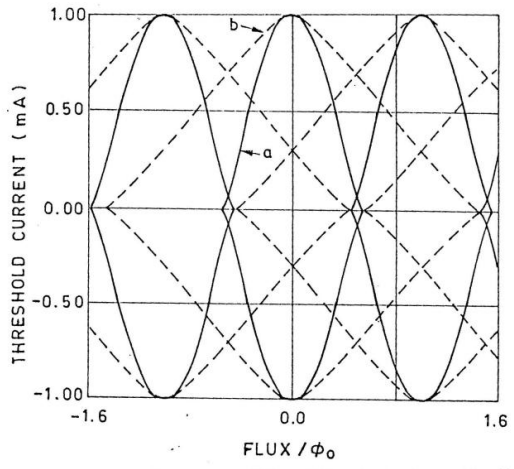

Fig.2 Threshold curves for two symmetric double – junction interferometer for (a) L = 0.2 pH, Io = 0.5 mA, giving β = 0.30 and (b) L = 4.0 pH, Io = 0.5 mA, giving β = 6.1.

$Io2 / Io1 + \beta << 1$ ----------(.8)

Egn.(7) has a solution for $\theta2$ only for a limited range of $\theta1$ (near $\pi/2$, $3\pi/2$, etc.). Setting $\theta1 = \pi/2$ and noting that Egn.(8) requires $\beta2 < 1$ ($\beta1$ is not required to small however), we get

$\theta2 = \phi x / \phi o + \beta1 + \pi/2$

Hence $Ig = Io1 + Io2 \cos(\phi x / \phi o - \beta1)$ ---------- (9a)

Which shows the sinusoidal behaviour.

Similarly with $\theta1 = -\theta2$ one gets

$Ig = - Io1 - Io2 \cos(\phi x / \phi o - \beta1)$ -(9b)

A symmetry interferometer can never exhibit sinusoidal behaviour (as shown Fig.1c) since it cannot satisfy Egn.(7).

This sinusoidal behaviour of the dc
SQUID is not useful for the logic and memory application. However, they may be useful for the rf power measurements [9].

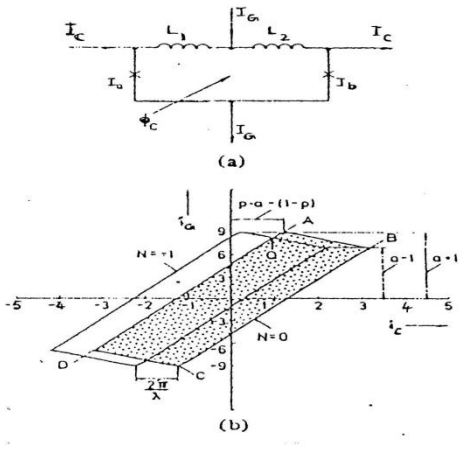

Fig. 3dc SQUID with two Josephson junctions A andB the total inductance L = L1 + L2 . (a) Equivalent circuit with gate current IG and the control current IC. (b) Threshold curves of flux quantum states IG = IG / Ib versus IC = IC / Ib for a = 8.0, $\lambda = 2\pi$, p = L1 / L = 0.25 and N = -1, 0.

An equivalent circuit of SQUID [10] is shown in Fig.3a. When the Josephson junction A and B are assumed to be point junctions, the maximum Josephson current ratio of the junctions A and B is a = Ia/Ib> 1. The total inductance between the junctions is L = L1 + L2. The insertion point of the gate current Ig is given by the tap ratio, p = L1/L. The control current Ic represents a transformed control current Ic' of a separate control line. The total flux in the interferometer is an integer multiple N of one flux quantum ϕo=2.07 mVps. Flux quantum states (FQS) exist within limited range in the current plane Ig, Ic. Their threshold curves are as functions of phase differences across the junctions θa and θb:

Ig = (a. sinθa + sinθb) . Ib --------(10a)

Ic = [(θa - θb + 2πN) / λ - (1 – p). sinθb + p.a sinθa]. Ib ---- (10b)

$$\theta_b = arc\cos\left(\frac{-a\cos\theta_a}{1+\lambda a\cos\theta_a}\right)$$ p = L_1 / L ; λ = 2π L. I_b ; $a = I_a / I_b$; $L = L_1 + L_2$ / ϕ_o

The curves depend on five magnitude parameters

i) The characteristic phase $\lambda = 2\pi L\ I_b/\phi_o$
ii) The maximum Josephson current of the smaller junction I_o
iii) The current ratio, a
iv) The tap ratio, p
v) The number of flux quanta N.

An example of two FQS in the normalized current plane with $i_G = I_g / I_o$ and $i_C = I_c / I_o$ is given in Fig.3b, for $\lambda = \pi$, a=8, p=0.25 and N=0, 1 [10].

For N = 0 mode, the points A and C are point symmetric with respect to the origin. The same is true for the points B and D. The currents at the points are given analytically [10].

A) $I_{gA} = (a+1)\ I_o$

$I_{cA} = (p.(a+1) -1).\ I_o$

B) $I_{gB} = (a-1)\ I_o$

$I_{cB}\ (\pi/\lambda + p.(a-1) + 1)\ I_o$

The control current shift is given by [10]

$\Delta I_c = \phi_o / (L_1 + L_2)$

which can also can be written as

$\Delta I_c = 2\pi\ I_o / \lambda$

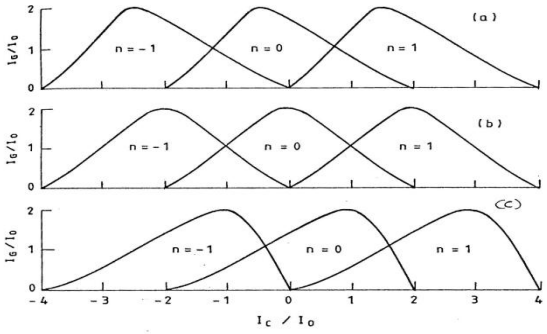

Fig. 4 Threshold characteristic of a dc SQUID obtained in terms of a device parameters. Fig. (a) – (c) shows the threshold characteristics of a dc SQUID for the same value of $\lambda = \pi$ but with different values of p = L_1 / L = 0.25, 0.50 and 1.0

The static characteristics of the SQUID have been obtained using Egns.(10a) and (10b). Fig. 4 shows the threshold curves of a dc SQUID obtained in terms of device parameters. Fig.4((a)-(c)) shows the threshold characteristics of a dc SQUID for the same value of $\lambda = 1.0\pi$, but with different value of p = L_1/L = 0.25, 0.50 and 1.0 respectively. It can be observed from Fig. 4 that for p = 0.5 the threshold curves are symmetric and in other cases the vortexes (lobes) are not symmetric with respect to their mid-points. For the memory application of SQUID, the vortexes preferably be symmetric with respect to their mid-points.

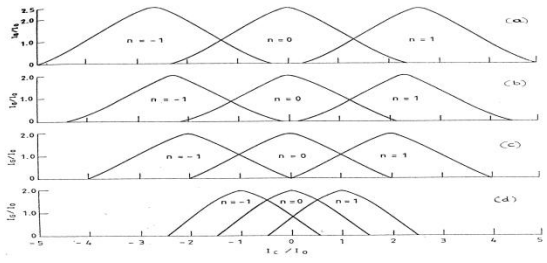

Fig.5 Threshold characteristic of dc SQUID obtained in terms of a device parameters. Fig. (a) – (d) shows the threshold characteristics of a dc SQUID for the same value of p = L_1/L

= 0.50 but with different values of λ = 0.75π, 0.87π, 1.0π and 2.0π.

In Fig.5 we have obtained the SQUID static characteristics for the same value of p = 0.5, but with different value of λ = 0.75π, 0.87π, I.0π and 2.0π. It is observed that as the value of λ increases, the lobes come closer and closer and thereby overlapping is more. The overlapping characteristics (Fig.5d) of the SQUID are not preferable for the memory application because of uncertainty in fixing the biasing point. So, for logic and memory applications, the dc SQUID parameters can be optimized at p = 0.5 and λ = 1.0π.

DYNAMIC RESPONSE OF THE SQUID:

In designing Josephson digital circuits, computer simulations of the static as well as of the dynamic device behaviour play an essential role because of the lack of sufficiently accurate analytical approximations. The dynamic description of the superconducting networks, containing Josephson tunnel junctions, self- and mutual -inductances, capacitances and resistors, results in a set of equations for the current continuity and zero-voltage sum and the particular current-voltage integral equations of the junctions.

IBM and Bell Labs have been adopting the standard electrical network analysis programs (for examples ASTAP [11], SPICE [12], etc) in order to obtain the circuit static as well as the dynamic response [13].

In the present case we have adopted a more general approach to obtain the dynamic response of SQUID. The dynamic equations of the SQUID have been taken and solved numerically by the Runge=Kutta method. In the switching dynamics of a logic gate, the high-frequency oscillation present in the load current with oscillation periods of a few ps stems from the oscillating supercurrent in the interferometer junctions. The frequency of these oscillations is related by to the actual junction voltage. Because these oscillations are still slow enough and can have sufficient energy to switch the following gate, they have to modelled accurately although the overall switching transient is in the tenths of ps. For an accurate computation of this oscillation, a minimum time-step size in the simulation of about 0.01 has to be used [13].

From Egns.(10a) and (10b) we can have,

$(1 - P)I_G + I_C = [(\theta_a - \theta_b + 2\pi N)I_o/\lambda + a\, I_o \sin\theta_a]$

In the dynamic case the above equation modifies to:

$$(1 - P)I_G + I_C = (\theta_a - \theta_b + 2\pi N)\, I_o /\lambda + a\, I_o \sin\theta_a + a\, \frac{\phi_o}{2\pi} C_j \frac{d^2\theta_a}{dt^2} + a\, \frac{\phi_o}{2\pi R_a} \frac{d\theta_a}{dt}$$

$$or\ \frac{d^2\theta_a}{dt^2} = \frac{2\pi}{\phi_o C_j a} [\, (1-p) I_G + I_C + (\frac{\theta_a - \theta_b - 2\pi N}{\lambda}) I_o - a\, I_o \sin\theta_a - \frac{a\,\phi_o}{2\pi R_a} \frac{d\theta_a}{dt} \quad \text{-------(11)}$$

Similarly,

$$\frac{d^2\theta_b}{dt^2} = \frac{2\pi}{\phi_o C_j b} [\, pI_G - I_C + (\frac{\theta_a - \theta_b + 2\pi N}{\lambda}) I_o + b\, I_o \sin\theta_b - \frac{b\,\phi_o}{2\pi R_b} \frac{d\theta_b}{dt} \quad \text{---------(12)}$$

Eqns. (11) and (12) are in the form of the second order differential equation. These equations can be solved by fourth – order Runge-Kutta method on a computer to obtain the dynamic response of the SQUID.

For a 2.5 μm Josephson junction technology, the material parameters used for designing the SQUID memory cell are given in Table-I.

Further, the SQUID memory cell is designed under the following conditions:

i) Line width and line spacing = 2μm

ii) Layer-to-Layer registration = 1.5μm.

With Wc = 7.0μm the derive area of the SQUID memory cell is 7μm x 16.5μm.

Using the parameters given in Table-II, the SQUID device parameters p = L_1/L = 0.5 and λ = 1.01 π (approximately).

The static characteristic of the SQUID memory cell can be obtained by substituting the device parameters in Eqns.(10a) and (10b).

4. SQUID AS A MEMORY CELL

The superconducting memory cell is mainly based on the principle of storing an information in a superconducting loop as a persistent ring current. This persistent ring current is accompanied by a magnetic flux which is quantized and is an integer multiple of the flux quantum, $\phi_o = \hbar/2e = 2.07\, x10^{-15}\, Vs.$

The vortex modes of an interferometer (SQUID) are superconducting states and the modes are distinguished by the number of flux quanta stored in them.

For L. I_o products larger than about $0.2\phi_o$ the vortex modes overlap one another considerably. This means that in the overlap region either of two superconducting states are possible, differing by just one flux quantum. It is this

bistable region which is well suited to store one binary bit of information. Storage into overlapping vortex modes was first theoretically [2] predicted and then experimentally [3] demonstrated for two-junction interferometers. Because they operate with single flux quanta, these storage devices are also known as single flux-quantum (SFQ) memory cells.

In the quiescent state, in order that stored information is not lost, the device has to be biased into an overlap region by an external magnetic field or by a dc-control current I_{cb}.

The two-junction SQUID offers some advantages over other devices for single-flux storage, (i) because all vortex modes have equal shape in this SQUID, the two storage states are equivalent, which has advantages with respect to operating margins (ii) the length-to-width ratio is more square than for long Josephson junctions, (iii) perhaps most important, the two-junction SQUID allows a read mode, which is probably difficult to achieve with other Josephson devices [4].

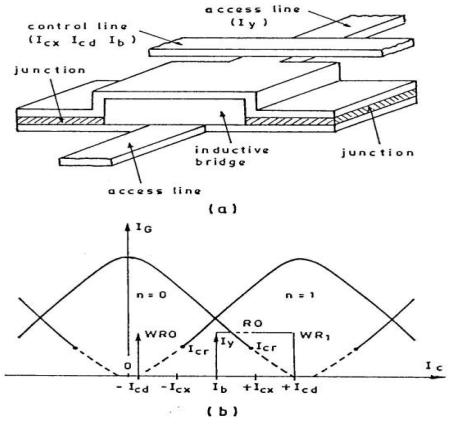

Fig. 6 (a) Basic structure of a Single – Flux – Quantum cell. The single control line shown here represent three lines in actual practice. (b) Threshold characteristic for the single-flux-quantum memory cell. Properties of the cell are chosen to overlap the modes with zero and one flux quantum in the cell.

For writing, the operation is made vortex-to-vortex transition as shown in the Fig.6. It is assumed that vortex states n=0 and n=1 are used for storing a '0' or '1' of the binary system, and further, that the SQUID is originally in the state n=0. If a vortex-mode boundary is crossed, then a transition can takes place, the nature of which depends on whether crossing occurs below or above a critical current I_{cr} (as shown in Fig.6). If the boundary is crossed at a value $I_y < I_{cr}$, then switching to another vortex mode occurs. This transition is used for writing. If however, the boundary is crossed at $I_y > I_{cr}$," then the cell switches to the voltage state. This transition is used for reading. For writing '1', positive currents I_{cx} and I_{cd} are first applied and then the current I_y.

The current trajectory goes from the overlap region into the mode n=1 and crosses the mode boundary below Icr. In this way, the cell swithches into the mode n=1 in which it remains stable after the selection currents have been swithced off.

For writing '0' (WRO), the polarity of the selection of currents I_{cx} and I_{cd} are reversed.

For reading, the current I_y is applied first followed by currents I_{cx} and I_{cd}, so that the current trajectory crosses the vortex boundary above the critical current. If the cell is in n=0 state, then it switches to the voltage state. If the cell is in n=1 state, the current trajectory stays within that mode and no switching occurs. In this way a '0'and a '1' can be distinguished.

The vortex transitions are very fast. The cell is static and in the storage state it consumes no power. However, for holding the information, the bias current I_b has to be permanently applied. As the Read out is destructive so after reading, the information has to be rewritten.

If I_g is large, when a vortex boundary is traversed, the device no longer switches into the vortex state but instead goes permanently to the voltage state. It only occurs if the SQUID is little damped by internal or external losses. The uses of the vortex-to-vortex transition for reading was proposed and experimentally shown in [2]. After reading, the cell has to be reset to the superconducting state by switching off I_g for a brief period. In the read process '1' state is destroyed and has to be rewritten.

The points P_{cL} and P_{cR} which mark the boundary between mode-to-mode transitions and mode-to-voltage-state transitions, are called critical points. Their properties, which are important in the mode operation, will be examined latter in detail. For the optimization of the cell design, it is also necessary to know the critical points (I_{cR} and I_{cL}) which depend on λ.

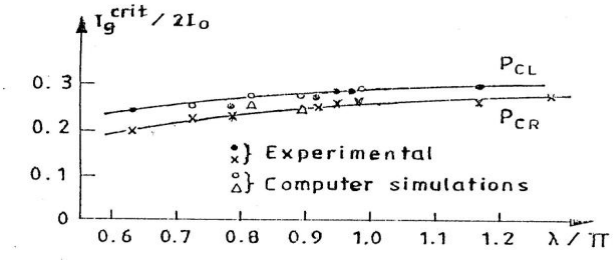

Fig. 7 Dependence of critical point λ/π. Comparision between experimental data and results of computer – simulation.

Fig.7 shows a set of measured data for the critical points P_{cL} and P_{cR} as a function of λ/π in the range of interest [26]. The slow increase of I_{gcrit} vs λ results from the increase of the device damping as increases.

It is clear that one would like to operate the cell in a high-impedance environment. This will bring the critical point down to a reasonable level (at about half the height of the overlap region) and make them more or less independent of loading. This will have the further advantage that cells which are series connected in a high-impedance string will be fairly well isolated from one another.

The critical points are confirmed by computer simulations of an interferometer model in which the junctions are represented by their distributed model [14].

A single flux quantum (SFQ) memory cell is expected to be used as the main memory in a Josephson supercomputer, because of its lower power consumption and high current density. So far, several types of SFQ memory cells have been proposed [14] [15]. Among them, the triple coincident SFQ memory cell proposed by Broom et at. [14] seems to be promising as a large scale memory circuit due to its wide operating margin and high stability.

H. Suzuki [16] has fabricated a SFQ memory cell with a 2-junction interferometer using Pb-alloy technology. Here we are designing theoretically the SFQ memory cell using Nb/A10 x/Nb Josephson technology, since this has several advantages over Pb-alloy technology.

DESIGN OF A MEMORY CELL:

The SFQ memory cell consists of a 2-junction bridge type interferometer. In designing the memory cell, it is necessary to obtain the threshold characteristic as a function of various device dimensions. The threshold characteristic can be calculated by solving equation derived from an equivalent circuit as shown in Fig.8.

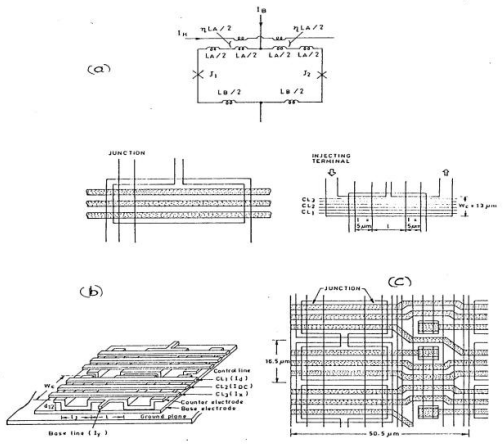

Fig. 8 Design criteria of the SFQ memory cell. (a) Equivalent circuit of the SFQ memory cell (b) Drawing of the memory cell with control lines. (c) Part of the designed SFQ memory cell.

In the calculations, estimated values of the inductances in the equivalent circuit play a key role. We have selected the same values of device parameters in designing the SFQ memory cell that are used in the case of the SQUID OR gate[17]. Basically there is no difference between the logic gate and SFQ memory cell except the mode of operation.

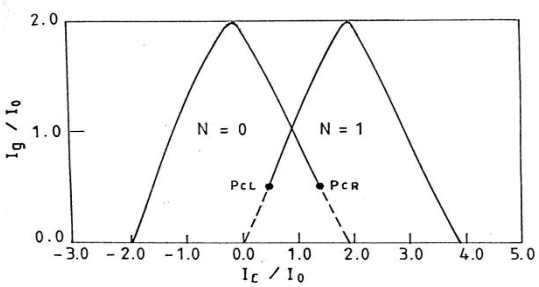

Fig. 9 Threshold characteristic of the designed SFQ memory cell. The parameters are p = 0.5, $\lambda = 1.0\ \pi$.

The critical points of the SFQ memory cell are obtained from Fig.7. The threshold characteristic of the designed memory cell is shown in Fig.9. The cell area is considered as 13.5μm x 20.5μm including the return lines which is less than the memory cell obtained by Suzuki [16].

DYNAMIC RESPONSE OF THE MEMORY CELL:

Fig.10 shows the dynamic response of the SFQ memory cell using Pb-alloy technology. The dotted curve shows the dynamic response of the WRITE operation whereas the solid curve indicates the dynamic response of the READ operation. It is apparent from the Fig.10 that time taken for WRITE "1" in the cell based on Pb-alloy technology is 50 ps and to READ "1" the cell is 30ps. These are very small compared to previous SFQ memory cells [4, 14].

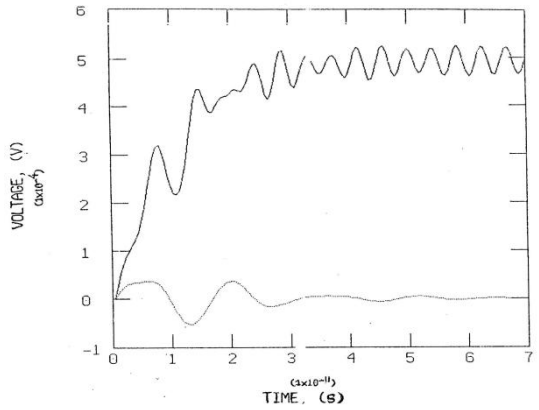

Fig. 10 Dynamic response of the SFQ memory cell using Pb-alloy technology. The dotted curve shows the dynamic response for WRITE operation, whereas solid curve indicates the dynamic response for READ operation

Fig.11 shows the dynamic response of the SFQ memory cell using Nb/A10x/Nb technology. The dotted curve shows the dynamic response of the WRITE operation whereas the solid curve indicates the dynamic response of the READ operation. It is apparent from the Fig.10 that time

taken for WRITE "1" in the cell based Nb/A10x/Nb technology is 20 ps and to READ "1" the cell is 15ps. These are very small compared to previous SFQ memory cells [4, 26]. The SFQ memory cell designed here is a destructive type. It can be made nondestructive by making the switching as a non-latching type. That means after reading, the cell will come back to its superconducting state (ON) state [18] [19].

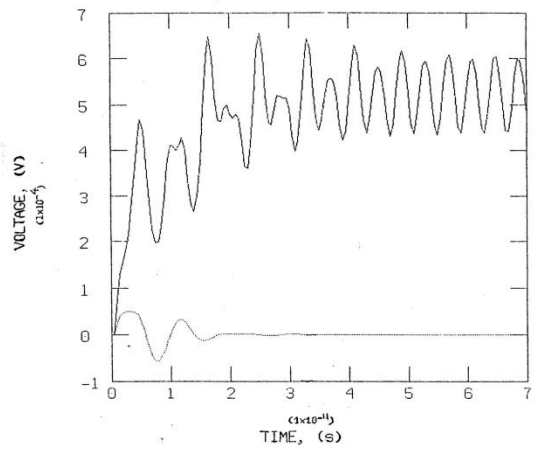

Fig. 11 Dynamic response of the SFQ memory cell using Nb/A10x/Nb technology. The dotted curve shows the dynamic response for WRITE operation, whereas solid curve indicates the dynamic response for READ operation.

5. CONCLUSIONS

In the present paper we have made an attempt to obtain the optimized parameters, properties and optimizations techniques of SQUID to be useful for the design of memory cells. For memory applications, it is found that the optimized device parameters are p = 0.5 and $\lambda = \pi$. However, for the SQUID used as an AND gate[17], the device parameters are obtained as p = 1.0 and $\lambda = \pi$, so that it provides large gain and operating margins. The logic and memory cell have been designed using these optimized techniques and the dynamic response of these have been obtained by computer-simulation. It is apparent from the simulation that the speed of the designed logic and memory cell is extremely high compared to earlier investigations. Further, the circuit dimension of the logic and memory cell is very low.

6. ACKNOWLEDGEMENTS

The greatest thanks to my guide ,Prof. Dr.J. C. Biswas, Ex-Professor, ECE Department , Indian Institute of Technology , India for his quality oriented suggestions made crucial impact on the value and importance of this work. I would like to acknowledge Prof.C.L.R.S.V. Prasad, Prinipal GMR Institute of Technology, Rajam, A.P,India for his constant encouragement to finish this work.

REFERENCES

1. T. R. Gheewala, " Josephson logic devices and circuits," IEEE Trans. Electron Devices vol. ED-27, no.10, October 1980, pp. 1857-1869.
2. P. Gueret, " Experimental observation of switching transients resulting from single flux-quantum transitions in superconducting. Josephson devices," Appl. Phys. Lett. vol.25, 1974, p.426.
3. P. Gueret, 'Storage and detection of a single flux quantum in Josephson-junction devices," IEEE Trans. Magnetics vol. MAG-11, 1975, p.751.
4. P. Wolf, " SQUIDS as computer elements," SQUIDs : Superconducting Quantum Interference Devices And Their Applications, H. D. Hahlbohrn and H. Lubbig (Eds.), Walter de Gruyter, Berlin, FRG, 1977, pp. 519-540.
5. T. A. Fulton, L. N. Dunkleberger and R. C. Dynes, " Quantum interference properties of double Josephson junctions," Phys. Rev. B vol.6, no.3, August 1972, pp. 855-875.
6. B. S. Landman, " Calculation of the threshold curves for Josephson interferometer devices," IEEE Trans. Magnetics vol.MAG-13, no.1, January 1977, p.871.
7. W. T. Tsang and T. VanDuzer, " do analysis of parallel arrays of two and three Josephson junctions," J. Appl. Phys. vol.46, no.10, October 1975, pp. 4573-4580.
8. R. L. Peterson and C. A. Hamilton, " Analysis of threshold curves for superconducting interferometers," J. Appl. Phys. vol.50, no.12, December 1979, pp. 8135-8142.
9. R. L. Peterson, " Sinusoidal response of dc SQUIDs for rf power measurements," J. Res. Nat. Bur. Stand. vol.92. no.A. July-August 1987, pp. 253-259.
10. J. Wunch, W. Jutzi and E. Crocoll, " Parameter evaluation of asymmetric interferometers with two Josephson junctions," IEEE Trans. Magnetics vol.MAG-18, no.2, March 1982, pp. 735-737.
11. ASTAP, IBM Advanced Statistical Analysis Program, IBM publication No. SH20-1118, available through IBM Branch office.
12. SPICE 2 Report, Version 2E0 1978, E. Cohen, A. Vladimirescer and 0. D. Pederson, Univ. of California, Dept. of Elect. Engg. and Computer Science.
13. H. Jackel, W. Bachtold, " Computer-simulation models for digital Josephson Devices and circuits," CIRCUIT ANALYSIS SIMULATION AND DESIGN, A. E. Rulhi (Ed.), Elsevier Science publishers B. V. (North-Holland), 1986, pp. 179-205.
14. P. Gueret, T. 0. Mohr and P. Wolf, " Single-flux quantum memory cells," IEEE Trans. Magnetics

vol.MAG-13, no.l, January 1977,pp. 52-55.

15. R. F. Broom, P. Gueret, W. Kotyczka, T. 0. Mohr, A. Moser, A. Oosenbreg and P. Wolf, " Model for a 15ns 16K RAM with Josephson junctions," IEEE J. Solid-state Circuits vol.SC-4, no.4, August 1979, pp.690-699.
16. H. Suzuki, ' Characteristics of Single Flux Quantum Josephson cells," Fujitsu Sci. Tech. J. vol.19, no.4, December 1983, pp. 475-496.
17. K.Srinivas," A Complete Approach of dynamic simulations of SQUID Logic gates and memory cells" Presented in Asian Conference on Applied Superconductivity and Cryogenics held on November 18-19, 2011 in New Delhi, India.
18. D. Drug and W. Jutzi, "Simulation of a NDRO memory cell with very small excess current Josephson junctions." Cryogenics, April 1984, pp.179-182.
19. H. Beha, " Dynamics of an asymmetric nondestructive read out memory cell," IEEE Trans. Magnetics vol.MAG-15, no-1, January 1979. pp.424-427.